J. Phycol. **59,** 167–178 (2023)

DOI: 10.1111/jpy.13302

TWO BLOOM-FORMING SPECIES OF *ULVA* (CHLOROPHYTA) SHOW DIFFERENT RESPONSES TO SEAWATER TEMPERATURE AND NO ANTAGONISTIC INTERACTION[1]

Ricardo Bermejo[3]

Department of Ecology and Geology, University of Malaga. Instituto Andaluz de Biotecnología y Desarrollo Azul (IBYDA), University Campus of Teatinos, E29010 Malaga, Spain

Maria Galindo-Ponce

Department of Biology, Faculty of Marine and Environmental Sciences, University of Cadiz, E11510, Puerto Real, Spain

Nessa Golden

Earth and Ocean Sciences, School of Natural Sciences and Ryan Institute, University of Galway, Galway H91 TK33, Ireland

Charlene Linderhoff

Botany and Plant Science, University of Galway, Galway H91 TK33, Ireland

Svenja Heesch[2]

CNRS, UMR 8227, Integrative Biology of Marine Models, Station Biologique de Roscoff, 29688 Roscoff cedex, France

Ignacio Hernández

Department of Biology, Faculty of Marine and Environmental Sciences, University of Cadiz, E11510, Puerto Real, Spain

and Liam Morrison[3]

Earth and Ocean Sciences, School of Natural Sciences and Ryan Institute, University of Galway, Galway H91 TK33, Ireland

The generalized use of molecular identification tools indicated that multispecific green tides are more common than previously thought. Temporal successions between bloom-forming species on a seasonal basis were also revealed in different cold temperate estuaries, suggesting a key role of photoperiod and temperature controlling bloom development and composition. According to the Intergovernmental Panel on Climate Change, water temperatures are predicted to increase around 4°C by 2100 in Ireland, especially during late spring coinciding with early green tide development. Considering current and predicted temperatures, and photoperiods during bloom development, different eco-physiological experiments were developed. These experiments indicated that the growth of *Ulva lacinulata* was controlled by temperature, while *U. compressa* was unresponsive to the photoperiod and temperatures assayed. Considering a scenario of global warming for Irish waters, an earlier development of bloom is expected in the case of *U. lacinulata*. This could have significant consequences for biomass balance in Irish estuaries and the maximum accumulated biomass during peak bloom. The observed seasonal patterns and experiments also indicated that *U. compressa* may facilitate *U. lacinulata* development. When both species were co-cultivated, the culture performance showed intermediate responses to experimental treatments in comparison with monospecific cultures of both species.

Key index words: **climate change; green tides; photoperiod; temperature; *Ulva compressa*; *Ulva lacinulata***

***Abbreviations*: ALTER, Alignment transformative environment software; BSA, Bovine serum albumin; dNTP, Nucleoside triphosphates containing deoxyribose.; DOC, Dissolved organic carbon; DON, Dissolved organic nitrogen; DOP, Dissolved organic phosphorus; DW_0, Dry weight at the beginning of the experiment; DW_f, Dry weight of seaweed at the end of the experiment; FW_0, Fresh weight at the beginning of the experiment; FW_f, Fresh weight of seaweed at the end of the experiment; IMTA, Integrated multitrophic aquaculture; IPCC, Intergovernmental panel on climate change; PhyDE, Phylogenetic data editor software; PRIMER 6,**

[1]Received 27 May 2022. Accepted 25 October 2022.
[2]Present address: Institute for Biological Sciences, University of Rostock, Albert-Einstein-Straße 3, D-18059, Rostock Germany
[3]Author for correspondence: e-mail ricardo.bermejo@uca.es; liam.morrison@universityofgalway.ie
Editorial Responsibility: J.M. Cock (Associate Editor)

Plymouth routines in multivariate ecological research software version 6.; RAxML, Randomized axelerated maximum likelihood; RGR, Relative growth rate; rY_C, Relative yield for *U. compressa*; rY_L, Relative yield for *U. lacinulata*; rY_T, Relative total yield; SST, Sea surface temperature; sY, Standardized biomass yield; t, Number of days; TIM3 + I + G, Transition model 3 + proportion of invariable sites + gamma distribution; U_x, Standardized nutrient uptake; X_0, Tissue nutrient content at the beginning of the experiment; X_f, Tissue nutrient content at the end of the experiment; Y_{ii}, Biomass yield of species "i" in monoculture; Y_{ij}, Biomass yield of species "i" co-cultured with species "j"; η^2_p, eta-squared method

The increase in human population, especially during the last 300 years (from 0.6 billion in 1700 to 7.9 billion in 2021; UN 2021), and the associated expansion and intensification of its activities (e.g., agriculture, fishing, fossil fuels burning, industry, marine transport, urbanization, and tourism), had led to important changes in the Earth's system, making humankind one of the most relevant drivers of global change (Camill 2010). Global warming and eutrophication are two processes mainly driven by anthropogenic activities, which are part of this global environmental change (Gattuso et al. 2015, Glibert 2017) and are considered among the most important threats to the conservation of aquatic ecosystems and their biodiversity (Lotze et al. 2006, Airoldi and Beck 2007, Coll et al. 2010).

During the last few decades, increases in mean sea surface temperatures (SST) have been recorded in cold and temperate locations around the world (Poloczanska et al. 2011, Bartsch et al. 2012, Casado-Amezúa et al. 2019) together with dramatic distributional shifts of many marine organisms, including key habitat-forming species and others of commercial interest (Wernberg et al. 2011, Casado-Amezúa et al. 2019). This trend is expected to continue during the 21st century, with a global sea surface temperature increase of 1.9°C during February and August, and maximum warming of around 4°C during spring and early summer at high latitudes of the northern hemisphere (Bartsch et al. 2012, IPCC 2021). In aquatic environments, this warming is expected to affect more significantly smaller and shallower water bodies such as estuaries and coastal lagoons, which show a lower thermal capacity and inertia as a result of their small size and high surface:volume ratio.

On the other hand, estuaries and coastal lagoons are the first recipients of pollutants via rivers in the land-to-sea pathway, this alongside their relatively small size makes these areas especially susceptible to pollution including nutrient over-enrichment. One of the most evident signs of nutrient over-enrichment is the development of macroalgal blooms (Valiela et al. 1997, Teichberg et al. 2010). Macroalgal blooms or seaweed tides are accumulations of a large biomass of fast-growing opportunistic seaweeds on shores and shallow waters as a consequence of their overgrowth (Fletcher 1996, Valiela et al. 1997, Smetacek and Zingone 2013). These blooms alter ecosystem functioning and structure, limiting the goods and services that estuarine and coastal environments provide (Costanza et al. 1997, Lotze et al. 2006, Airoldi and Beck 2007). Although macroalgal blooms are not toxic per se, many detrimental effects associated with their sheer physical mass or the degradation of large amounts of biomass have been described in human activities and wildlife (Krause-Jensen et al. 2008, Lenzi et al. 2012). The accumulation of layers of seaweed biomass on the shore and shallow waters, physically obliterates other coastal life and may prevent the use of these waters for many purposes (e.g., fishing, navigation, and tourism; Smetacek and Zingone 2013). The subsequent degradation of large amounts of seaweed biomass can lead to dystrophic crises, alter biogeochemical cycling, and produce unpleasant odors and the release of toxic compounds causing serious amenity and public health concerns (Teichberg et al. 2010, Smetacek and Zingone 2013).

The occurrence of seaweed tides is a widespread phenomenon affecting coastal areas all over the world (Lavery et al. 1991, Hernandez et al. 1997, Nelson et al. 2003, Wang et al. 2015, Allanson et al. 2016). Seaweed tides became more frequent and larger at the end of the 20th century, especially in industrialized countries. Since then, the number of reports from new locations and the magnitude of these tides have continued to increase (Valiela et al. 1997, Smetacek and Zingone 2013, Le Moal et al. 2019). Despite the critical role of nutrient over-enrichment in the occurrence of seaweed tides, additional abiotic and biotic factors such as light, temperature, local hydrodynamic conditions, grazing, propagule bank size, and local species pool or strains can be critical in explaining bloom development (Worm et al. 1999, Nelson et al. 2008, Fort et al. 2020). In this sense, the diversity of species with different ecological requirements capable of producing a bloom can increase the extension and persistence of seaweed tides throughout temporal and spatial successions (Lavery et al. 1991, Nelson et al. 2008, Bermejo et al. 2019, 2020).

Species of the genus *Ulva* are the main Chlorophytes responsible for green seaweed tides (Valiela et al. 1997, Smetacek and Zingone 2013, Wang et al. 2015). These species have a simple morphology, consisting either of a monostromatic tubular thallus (formerly *Enteromorpha* genus) or a distromatic laminar thallus (Hayden et al. 2003). Some *Ulva* species can display both morphotypes (Guidone et al. 2013) or show a high morphological variability depending on environmental conditions (Gao et al. 2016b). The high plasticity that these

species can show and the lack of reliable traits, especially in detached specimens, hinder accurate morphological identification (Malta et al. 1999, Guidone et al. 2013, Steinhagen et al. 2019). As a consequence of the difficulties in morphological identification, the study of the species composition and its importance in the development of these blooms has remained overlooked for long. However, the development of new molecular identification tools allows us to overcome these taxonomic challenges (Kang et al. 2019, Steinhagen et al. 2019, Fort et al. 2021) and suggests that multispecific green tides are more common than previously thought (Nelson et al. 2008, Guidone and Thornber 2013, Bermejo et al. 2019).

Irish green tides are multispecific and they are dominated by three main species (*Ulva compressa*, *U. prolifera*, and *U. lacinulata*—incorrectly known as *U. rigida* in Bermejo et al. 2019; see Hughey et al. 2022). The composition and dominance patterns of the main species forming green tides change seasonally, with proliferations dominated by tubular morphologies (i.e., *U. compressa* and *U. prolifera*) at the beginning of the bloom, and co-dominated by tubular (i.e., *U. compressa* and *U. prolifera*) and laminar (i.e., *U. lacinulata*) morphologies at the end (Bermejo et al. 2019; Fig. 1). The occurrence of temporal or spatial successions is usually indicative of different eco-physiological requirements (Fong et al. 1996, Lotze and Schramm 2000, Nelson et al. 2008). On this matter, a change in environmental conditions could lead to a shift in the composition and structure of the bloom (Lavery et al. 1991), which can have implications for ecosystem functioning (e.g., differences in decay and grazing rates, differential effects of tidal currents in biomass exportation; Coffaro and Bocci 1997, Nelson et al. 2008, Bermejo et al. 2019).

Light and temperature are the main factors explaining seasonal patterns of primary producers in temperate and polar environments (Lüning 1990, Bermejo et al. 2019). As these factors covariate, the development of factorial experiments is necessary to disentangle the contribution of each of them to explain the observed seasonal patterns, which is paramount to predicting the responses of primary producers to ongoing global warming. Furthermore, the assessment of species interaction, their ecological requirements, and the effects of biodiversity in the response of macrophyte assemblages to environmental pressures can be useful to understand their resilience or resistance in a global change scenario.

Thus, considering the current context of global change and the multispecific composition of Irish *Ulva* blooms, an experiment was performed in order to disentangle the effects of light and temperature on the growth of two main species of *Ulva* forming green tides (i.e., *U. compressa* and *U. lacinulata*) in cold temperate estuaries from the northern hemisphere and to assess the biotic interactions between the two species.

MATERIALS AND METHODS

"Ulva" identification, collection, and acclimation. Specimens of *Ulva compressa* and *U. lacinulata* were collected from the Clonakilty estuary, a eutrophic estuary located on the southwestern coast of Ireland which is affected by large and persistent macroalgal blooms of *Ulva* spp. and *Gracilaria vermiculophylla* (Wan et al. 2017, Bermejo et al. 2020, 2022). Thalli were transported to the laboratory wrapped in wet tissue inside a cooler box. There thalli were washed with 0.45 μm filtered seawater to remove sediment, organic debris, and epibiota. Specimens of *U. compressa* and *U. lacinulata* showing a healthier visual aspect and texture were sorted and identified based on morphological traits following Brodie et al. (2007). Furthermore, four specimens of *U. compressa* and five specimens of *U. lacinulata* identified based on morphological traits were selected to confirm the taxonomic identity using genetic barcoding (Fig. S1 in the Supporting Information).

Regarding the genetic barcoding, the large subunit of the gene that encodes ribulose bisphosphate carboxylase-oxygenase (RuBisCO; *rbc*L) was employed to genetically identify the samples. Whole-genomic DNA was extracted using the NucleoSpin® Plant II kit (Macherey-Nagel, Germany) according to the manufacturers' instructions. Polymerase chain reactions (PCRs) were prepared as follows: each reaction of 25 μL volume contained 12.375 μL sterile water, 5 μL 5x Green Go*Taq* Flexi buffer (Promega, France), 2 μL 25 mM $MgCl_2$, 0.5 μL 40 mM dNTPs, 0.5 μL BSA solution, 1 μL each of 10 uM forward and reverse primers, 0.125 μL Go*Taq* Flexi Polymerase (Promega, France), and 2.5 μL template DNA. The marker *rbc*L was amplified using primers SH_F1 and SH_R4 (Heesch et al. 2009) and internal primers (Hughey et al. 2019), respectively. Protocols for PCR amplification and purification of the products are given in Heesch et al. (2016). PCR products were Sanger sequenced, using the same primers, by a commercial sequencing service (Eurofins Genomics, Germany).

Sequences were checked by eye in 4Peaks v.1.7.2 (Griekspoor and Groothuis 2015) and included in an alignment of published sequence data (see Fig. S1 for GenBank accession numbers and references) in PhyDE version 0.9971 (Müller et al. 2010). The alignment of 1250 bp length contained 74 sequences, with *Gemina letterstedtioidea* serving as an outgroup. The online tool ALTER (ALignment Transformative EnviRonment; Glez-Peña et al. 2010) was used to transform the alignment before running the phylogenetic analysis in RAxML (Stamatakis 2014, Kozlov et al. 2019) using a graphic user interface (raxmlGUI 2.0; Edler et al. 2021). After running Modeltest implemented in RAxML (Darriba et al. 2020), the data set was analyzed based on the maximum-likelihood criterion using the TIM3 + I + G model, with bootstrap support estimated based on 1000 repetitions. The resulting phylogenetic tree was visualized in FigTree v1.4.3 (Rambaut 2016) and edited in Inkscape (https://inkscape.org/). Sequences are available in GenBank/ENA under accession numbers: OP555968-OP555976.

Specimens of the two species were cultivated separately using two 15 liters aquaria for 1 month in artificial seawater at a salinity of 32 (Coral Pro Salt, Red Sea) enriched with 1:2 diluted f/2 media without silicate (Guillard 1975). Aquaria were illuminated by white cool fluorescents tubes (Blau Aquaristic Lumina 1080) in a 15:9 h light:dark cycle at 80–90 μmol photons · m^{-2} · s^{-1}. The water temperature was set to 15°C using an aquaria cooler (TK 150, TECO®). To avoid

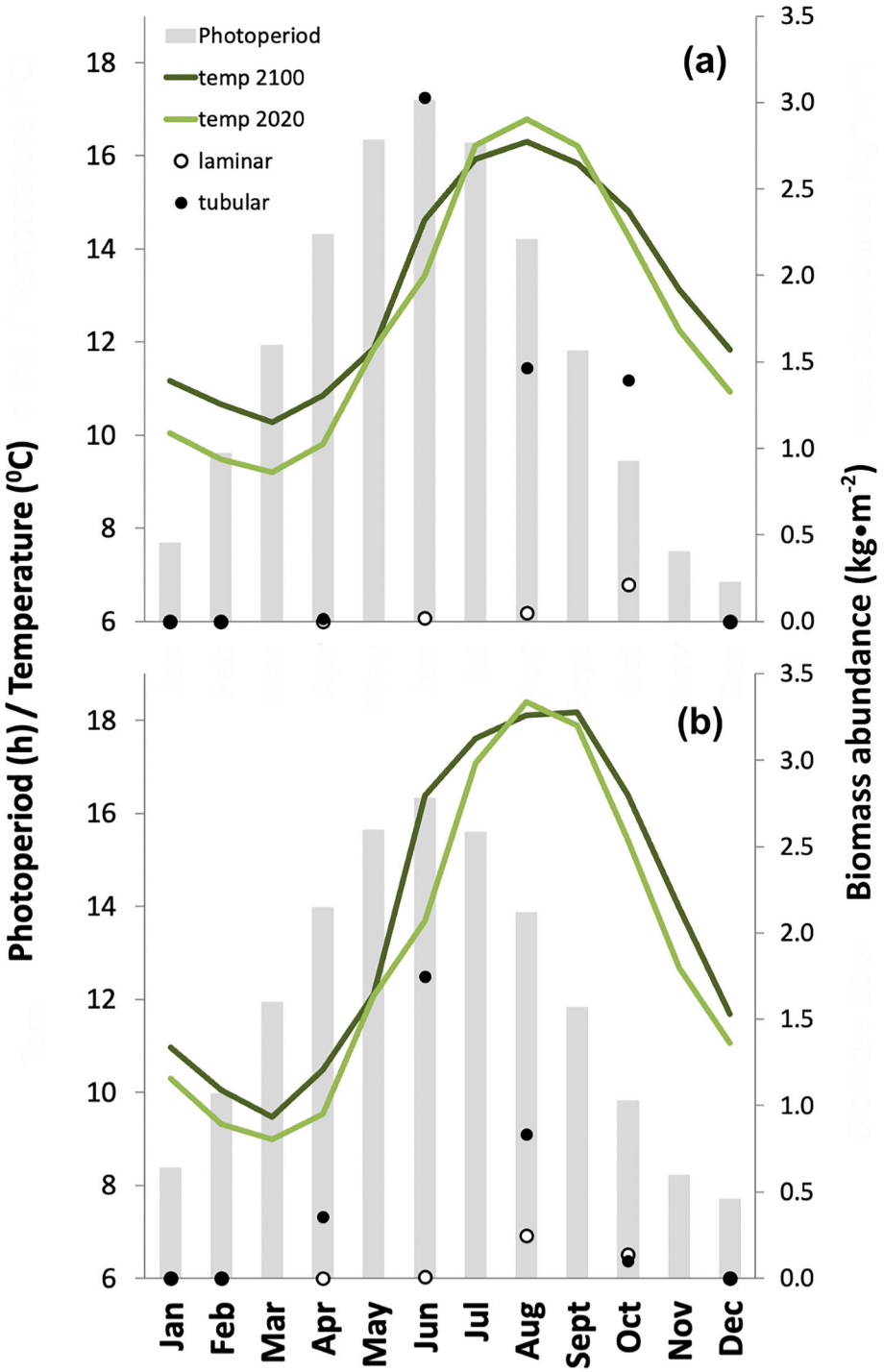

FIG. 1. Monthly *Ulva* biomass abundance (dots), photoperiod (bars), and sea surface water temperature (lines) for the Argideen (a) and Tolka (b) estuaries. Mean biomass abundances were extracted from Bermejo et al. (2019) and Bermejo et al. (2022) for the years 2016 and 2017. Photoperiod data were obtained from the Met Eireann website. Mean monthly sea surface temperatures for adjacent coastal waters for both estuaries for the years 2020 and 2100 were sourced from IPPC (2021) predictions. [Color figure can be viewed at wileyonlinelibrary.com]

bacterial growth and nutrient limitation, nutrient-enriched seawater was changed once a week, and a water pump was used in each aquarium to ensure constant water motion.

Experimental set-up. To determine the eco-physiological performance and to assess the biological interaction between *Ulva compressa* and *U. lacinulata* under different conditions of temperature and photoperiod, a factorial design was followed. Conditions were established considering current and future seawater surface temperature predictions for North East Atlantic coastal waters (IPCC model scenario A2), as well as the seasonal biomass dynamics, observed in Irish green tides (Fig. 1; Bermejo et al. 2019, 2022). According to these

observations, tubular morphologies of *Ulva* showed the peak of biomass during June, when the photoperiod was 16:8 h (light:dark) and mean water temperature was around 13 and 14°C. In the case of laminar morphologies, the annual maximum of biomass was observed during August, when the day length was 14 h and night length 10 h. Mean SST during this month ranged between 17 and 18°C. Regarding IPCC predictions for North East Atlantic waters, the most important monthly temperature anomalies are expected to occur during late spring and early summer, with an expected increase in mean SST of 3 or 4°C at the end of the XXI century (approx. 17°C expected for June 2070–2100). No or little temperature variation is expected for August. To identify the type of biotic interaction between the two species of *Ulva*, they were cultivated alone (monoculture; i.e., 100% initial biomass) and together (co-culture; 50% *U. compressa* + 50% *U. lacinulata* of initial biomass). Therefore, a factorial design was followed considering two temperatures (13.5°C and 17°C), two photoperiods (16:8 h and 14:10 h light:dark), and two culture conditions (monospecific and co-culture).

The experiments lasted for 10 d and all treatments and replicates were performed simultaneously. Seaweeds were incubated at an initial density of 0.2 $g \cdot L^{-1}$. Only specimens in a healthy vegetative condition (not reproductive or full of starch grains) were used. Four replicates were run per treatment. Each replicate consisted of a 500-mL glass beaker filled with half-strength f/2 media without silicate at a salinity of 32. The media were replaced every 2 days to avoid bacterial growth and nutrient limitation. The light was supplied from the top by white cool fluorescent tubes (Blau Aquaristic Lumina 1080), providing 80–90 μmol photons $\cdot m^{-1} \cdot s^{-1}$. This irradiance was chosen based on the light intensities reported by Vergara et al. (1997) and Wang et al. (2012) from submersed *Ulva* blooms. Beakers were placed in water-filled baths connected to different aquaria coolers (TK 150, TECO®) to maintain the temperature conditions. The position of the beakers was changed twice daily to ensure homogenization of light and temperature, during this procedure beakers were also shaken to provide agitation to facilitate nutrient uptake and limit the accumulation of oxygen. Irradiance, salinity, and water temperature were monitored daily. Irradiance was measured using a spherical underwater quantum sensor (LiCor-LI193SA) connected to a data logger (LICOR L1-1500). In the case of salinity and water temperature, a portable multiparametric sonde (sensION+; HACH©) was used. No significant deviations from experimental conditions were observed during the monitoring of experimental factors.

Growth rates, elemental composition, biomass yield, and nutrient uptake. Relative growth rate: The relative growth rate (RGR) was calculated assuming an exponential growth (equation 1). The fresh weights before and after the incubation period were measured using a precision weight scale accurate to 0.0001 g. The weights were recorded to the nearest 0.001 g. Before weighing, the specimens were gently blotted with filter paper until wet spots disappeared.

$$\mathrm{RGR}\left(d^{-1}\right) = ln(FW_f/FW_0)/t \quad (1)$$

where FW_f is the fresh weight of seaweed at the end of the experiment; FW_0 is the fresh weight at the beginning of the experiment; and t is the number of days.

Elemental composition: Seaweed tissue was freeze-dried and ground into a homogeneous powder using a TissueLyser II (QIAGEN) and tungsten balls. Samples were stored in a desiccator with silica gel until sent to "Servizos de Apoio á Investigación" at the University of La Coruña (Spain), where tissue C and N contents were determined using a Flash combustion EA1108 elemental analyzer (Carlo Erba Instruments).

Standardized biomass yield, and nitrogen and carbon uptake: The standardized biomass yield (sY) was calculated following equation 2. In the case of nitrogen and carbon uptake, equation 3 was used.

$$sY = (FW_f–FW_0)/(FW_0{}^*t) \quad (2)$$

$$U_x\left(mg \cdot g^{-1} \cdot d^{-1}\right) = (DW_f{}^*X_f–DW_0{}^*X_0)/(DW_0{}^*t) \quad (3)$$

where U_x is the standardized nutrient uptake; X_f is the tissue nutrient content at the end of the experiment; X_0 is the tissue nutrient content at the beginning of the experiment; DW_0 is the dry weight of seaweed at the beginning of the experiment; and DW_f is the dry weight of the seaweed at the end of the experiment.

Relative biomass yield: The relative yield for *Ulva compressa* (rY_C) and *U. lacinulata* (rY_L) were estimated from the initial and final fresh weight of each sample at the different treatment combinations, according to equation 4 (Bi and Turvey 1994, Leal et al. 2020).

$$rY_i = Y_{ij}/Y_{ii} \quad (4)$$

where Y_{ij} is the biomass yield of species "i" co-cultured with species "j"; Y_{ii} is the biomass yield of species "i" in monoculture.

The total relative yield (rY_T) for each sample was calculated as the sum of the relative yield of *Ulva. compressa* and *U. lacinulata* (equation 5).

$$rY_T = rY_C + rY_L \quad (5)$$

Values of $rY_T = 1$ imply neutral interaction, $rY_T > 1$ indicates a synergistic interaction, and $rY_T < 1$ indicates a mutual antagonism (Bi and Turvey 1994, Leal et al. 2020).

Statistical analyses. Biological performance of Ulva *spp.*: A three-way factorial analysis of variance (ANOVA) was used to test the effects of photoperiod (two levels), temperature (two levels), and the interspecific interaction with the other species (two levels) on the RGR and the elemental composition (i.e., C and N) of *Ulva compressa* and *U. lacinulata*. All variables were accomplished with normality and homoscedasticity assumptions according to Shapiro–Wilks and Levene tests except tissue N content of *U. lacinulata*, which did not accomplish with homoscedasticity even after data transformation. In this case, a permutational analysis of variance (PERMANOVA) based on Euclidean distances between samples was performed to confirm the statistical significance yielded by the traditional ANOVA test. A post hoc Tukey's test was used to compare between levels of factors when showing a significant effect.

Interaction between Ulva compressa *and* U. lacinulata: In the case of the relative yield of co-cultures, one-sample t-tests were performed to identify when the relative yield was different from 1 for rY_T or 0.5 for rY_C and rY_L (i.e., the expected rY_x assuming neutral interaction). When data did not accomplish the normality assumption, a one-sample Wilcoxon signed-rank test was used instead.

Culture stability: A one-way ANOVA was performed to assess the effects of the four different treatments on the biomass yield, N uptake, and C uptake of monocultures of *Ulva compressa*, *U. lacinulata*, and the co-culture of both species. All data were accomplished with normality and homoscedasticity. Based on ANOVA results, the effect size of the experimental treatment was determined following the "eta-squared" method (η^2_p) for each of the different variables to estimate the magnitude of the treatments on co-culture and monocultures performance (Lakens 2013). As a proxy of stability,

Levene's test was also assessed between the different cultures, pooling experimental conditions, to assess the homogeneity of variance for the variables considered (i.e., biomass yield, N uptake, and C uptake).

All statistical analyses were conducted using the software R version 3.2.1 (R Core Team 2017) and PERMANOVA+ add-on PRIMER 6 (Plymouth Routines in Multivariate Ecological Research) software. The significance level was set at 5% probability.

RESULTS

Biological performance of Ulva compressa. The ANOVA results (Table 1) indicated only a marginal effect (*P*-value = 0.10) of photoperiod on the growth of *Ulva compressa*. This species tended to grow faster under 16:8 h light:dark ($0.072 \pm 0.015 \cdot d^{-1}$) than under 14:10 L:D regime ($0.062 \pm 0.016 \cdot d^{-1}$; Fig. 2) and evidenced an RGR ranging from 0.020 to $0.095 \cdot d^{-1}$.

No effect of any factor was observed for tissue C content (Table 1). The mean tissue C content was $32.45 \pm 1.07\%$, with a minimum of 30.76% and a maximum of 34.44%. Regarding tissue N, a significant effect of temperature and its interaction with photoperiod were observed (Table 1). Values of tissue N content ranged between 4.15 and 5.33% and were relatively similar between treatments (maximum differences approximately 0.1 fold; Fig. 2), with maximum contents observed at 13.5°C for both photoperiods (4.90 ± 0.30 %N at 16:8 h light:dark; 4.82 ± 0.20 %N at 14:10 h light:dark) and minimum at 17°C and 16:8 h light:dark (4.47 ± 0.25 % N). Replicates at temperatures of 17°C and 14:10 h light:dark yielded intermediate tissue N contents (4.79 ± 0.20 %N). In all cases, the tissue N was clearly higher than the critical quota estimated for *Ulva* in previous studies (approx. 2.5 %N) indicating no nitrogen limitation.

Biological performance of Ulva lacinulata. Unlike what was observed for *Ulva compressa*, the ANOVA results revealed a significant effect of the factors co-culture and temperature on the growth of *U. lacinulata* (Table 2). No effect on growth was observed for photoperiod or any interaction among factors. The RGR of this species varied between 0.107 and $0.168 \cdot d^{-1}$. *Ulva lacinulata* grew faster in the presence of *U. compressa* and at warmer temperatures (maximum differences approximately 0.25-fold; Fig. 2). Maximum growth rates were observed at 17°C when co-cultured with *U. compressa* ($0.147 \pm 0.013 \cdot d^{-1}$) and minimum at 13°C in monospecific cultures ($0.117 \pm 0.006 \cdot d^{-1}$). Intermediate RGR was observed at 17°C in monoculture ($0.128 \pm 0.009 \cdot d^{-1}$) and 13.5°C when cultured with *U. compressa* ($0.134 \pm 0.010 \cdot d^{-1}$).

Regarding tissue N content, values ranged from 4.11 to 4.86%. Significant differences were found between temperatures, with higher contents at 13.5°C ($4.52 \pm 0.2\%$) than at 17°C ($4.37 \pm 0.09\%$). In all cases, tissue N was higher than the critical quota indicating again no nitrogen limitation during the development of this study. No effect of any factor was observed for tissue C content (Table 2). The mean tissue C was 32.15 ± 0.87 %C, with a minimum value of 30.38% and a maximum of 33.38%.

Biological interaction between Ulva compressa *and* U. lacinulata. Regarding *Ulva compressa*, the observed relative yield when cultivated with *U. lacinulata* (1:1 initial proportion) was generally similar to the expected one assuming no effect of *U. lacinulata* in *U. compressa* (i.e., 0.5). However, when cultivated at 13.5°C and 14:10 h light:dark photoperiod, the observed relative yield for *U. compressa* was significantly higher than the expected one (one-sample *t*-test; $t_3 = 3.257$, *P*-value = 0.0236), suggesting an enhanced yield of *U. compressa* when cultured with *U. lacinulata* (Fig. 2). The observed relative yield for *U. compressa* ranged from 0.45 ± 0.23 (14:10 h light:-dark and 17°C) to 0.56 ± 0.04 (14:10 h light:dark and 13.5°C).

In all the experimental conditions assayed, the observed relative yield of *Ulva lacinulata* in co-culture with *U. compressa* was greater than the expected one assuming no effect of this species on *U. lacinulata* (one-sample *t*-tests; $t_3 > 2.36$, *P*-values <0.05). The observed relative yield of this species varied between 0.58 ± 0.06 (16:8 h light:dark and 13.5°C) and 0.73 ± 0.09 (14:10 h light:dark and 13.5°C). This is shown by the "^" shape of the increase in the relative yield of *U. lacinulata* with its proportion in co-culture in the replacement diagrams (Fig. 3), indicating a positive effect of *U. compressa* in the yield of *U. lacinulata*.

Although the relative yield of *Ulva lacinulata* was enhanced in all experimental conditions and no negative effect of *U. lacinulata* in the yield of *U. compressa* was observed (Fig. 3), a significant increase in the total relative yield of the culture was only observed at 13.5°C and 14:10 h light:dark photoperiod (one-sample *t*-test; $t_3 = 10.144$, *P*-value = 0.001).

TABLE 1. Results of the three-way ANOVA assessing the effects of the factors "Biotic Interaction" (BI), "Photoperiod" (Phot), and "Temperature" (Temp) on the relative growth rate (RGR), tissue C and N content of *Ulva compressa*.

		RGR		Tissue C content		Tissue N content	
	Df	MS	*F*-value	MS	*F*-value	MS	*F*-value
BI	1	0.05	0.02	0.12	0.08	0.10	1.62
Phot	1	7.86	2.80	0.47	0.33	0.12	1.88
Temp	1	0.81	0.29	0.95	0.67	0.41	6.44*
BI x Phot	1	0.43	0.15	0.00	0.00	0.03	0.45
BI x Temp	1	2.31	0.82	0.02	0.01	0.01	0.08
Phot x Temp	1	0.00	0.00	0.01	0.01	0.32	5.03*
BI x Phot x Temp	1	0.03	0.01	0.11	0.08	0.00	0.00
Residuals	24	2.81		1.42		0.06	

Note: * *P*-value <0.05; ** *P*-value <0.01; *** *P*-value <0.001.

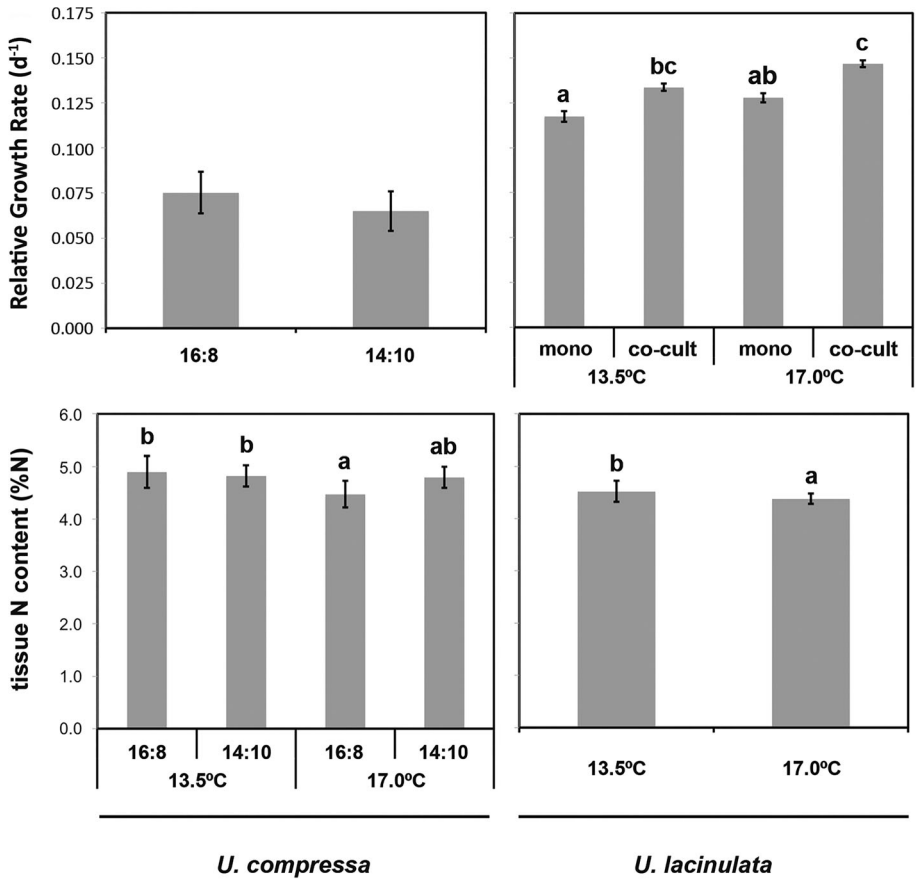

FIG. 2. Relative growth rate and tissue N content of *Ulva compressa* and *U. lacinulata* according to factors or combination of factors that showed a significant or marginal effect in the ANOVA. Data represent mean ± standard deviation. Letters over the bars represent significant differences between treatments according to the Tukey test. Further information is in Table S1 in the Supporting Information.

TABLE 2. Results of the three-way ANOVA assessing the effects of the factors "Biotic Interaction" (BI), "Photoperiod" (Phot), and "Temperature" (Temp) on the relative growth rate (RGR), tissue C and N content of *Ulva lacinulata*.

		RGR		Tissue C content		Tissue N content	
	Df	MS	*F*-value	MS	*F*-value	MS	*F*-value
BI	1	24.78	25.64***	0.46	0.67	0.06	2.35
Phot	1	0.02	0.02	0.98	1.42	0.01	0.22
Temp	1	11.05	11.44**	1.21	1.74	0.16	6.30*
BI x Phot	1	1.93	2.00	1.80	2.61	0.00	0.08
BI x Temp	1	0.15	0.15	1.85	2.67	0.07	2.78
Phot x Temp	1	0.93	0.96	0.82	1.18	0.00	0.06
BI x Phot x Temp	1	0.27	0.28	0.06	0.09	0.00	0.11
Residuals	24	0.97		0.69		0.03	

Note: **p*-value <0.05; ** *P*-value <0.01; *** *P*-value <0.001.

Under this experimental condition, the obtained yield was 30% higher than expected. The observed total relative yield ranged from 1.06 ± 0.12 (16:8 h light:dark and 13.5°C) to 1.29 ± 0.06 (14:10 h light:dark and 13.5°C).

Culture stability. No significant effects of treatment were observed for the biomass yield and nitrogen and carbon uptake of 1:1 co-cultures and *Ulva compressa* monocultures (Fig. 4). The effect size of experimental treatment ranged from 0.039 to 0.079 for *U. compressa*, and from 0.096 to 0.29 for the co-cultures. By contrast, *Ulva lacinulata* cultures showed significant differences between treatments in the biomass yield ($F_{3,12}$ = 3.879; *P*-value = 0.038; η^2_p = 0.49), nitrogen uptake ($F_{3,12}$ = 5.296; *P*-value = 0.015; η^2_p = 0.57), and carbon uptake ($F_{3,12}$ = 5.888; *P*- value = 0.0104; η^2_p = 0.59). Cultures of this species yielded the highest biomass yields and nitrogen and carbon uptakes, whereas *U. compressa* the lowest (Fig. 4). In the case of *U. lacinulata*, the biomass yield ranged from 0.192 to 0.289 $g \cdot g^{-1} \cdot d^{-1}$, the nitrogen uptake from 9 to 15 $mg\ N \cdot g^{-1} \cdot d^{-1}$, and the carbon uptake from 67 to 112 $mg\ C \cdot g^{-1} \cdot d^{-1}$. Regarding *U. compressa*, the biomass yield was comprised between 0.040 and 0.138 $g \cdot g^{-1} \cdot d^{-1}$, the nitrogen uptake between 1 and 9 $mg\ N \cdot g^{-1} \cdot d^{-1}$, and the carbon uptake

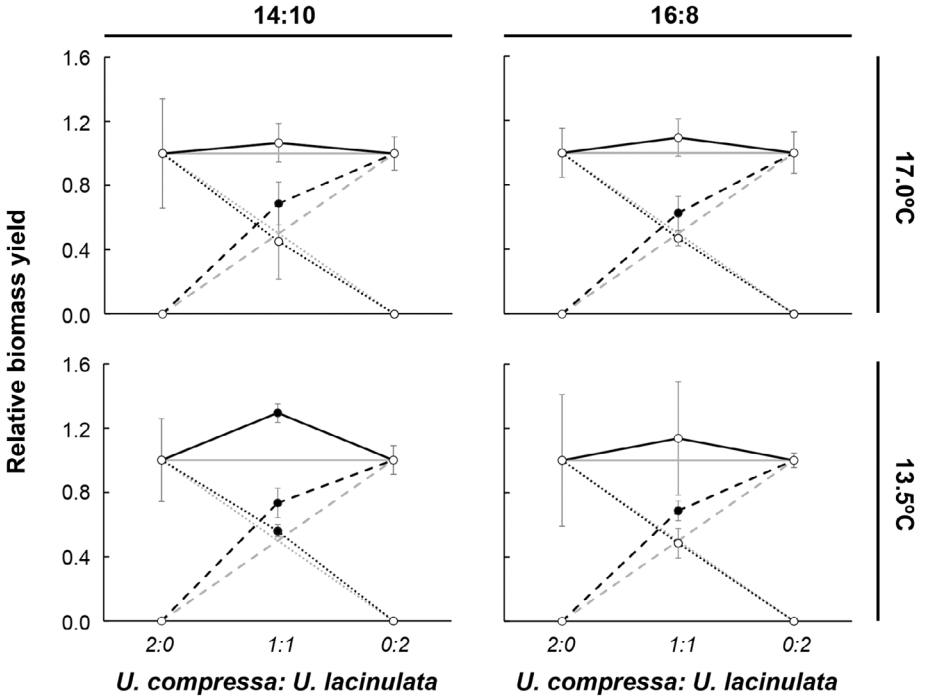

FIG. 3. Relative yield of *Ulva compressa* (dotted line), *U. lacinulata* (dashed line), and total (solid line) under the four different conditions assayed. Data represent mean ± standard deviation ($n = 4$). Black symbols indicate significant differences between observed and expected values according to the one-sample t-test; white symbols indicate non-significant differences. Black lines represent observed trends, and gray lines depicted expected trends assuming neutral interactions between species.

between 6 and 68 mg C · g^{-1} · d^{-1}. The yield of the co-cultures varied between 0.155 and 0.281 g · g^{-1} · d^{-1}, the nitrogen uptake between 7 and 11 mg N · g^{-1} · d^{-1}, and the carbon uptake between 44 and 84 mg C · g^{-1} · d^{-1}. Pooling all treatments, Levene's test indicated no significant differences on the homogeneity of variances between the different cultures and variables ($F_{11,36} < 0.9607$; *P*-values >0.45).

DISCUSSION

The results indicated that, during Irish summer conditions, temperature controls the development of *Ulva lacinulata* (Table 2), while photoperiod might play a more important role in triggering the growth of *U. compressa* (Table 1; but note that only a marginal effect was observed). These findings partially explain the seasonal patterns found in Irish estuaries (Jeffrey et al. 1995, Bermejo et al. 2019, 2022), with the most important increase in biomass of tubular (i.e., *U. compressa* and *U. prolifera*) morphologies occurring during the months of longer photoperiods, and the most important accumulation of laminar *Ulva* (i.e., *U. lacinulata*) when water temperature increases in mid-summer. Nevertheless, important differences in growth were observed between species, with *U. lacinulata* displaying a higher relative RGR than *U. compressa* (0.123 ± 0.009 · d^{-1} and 0.067 ± 0.016 · d^{-1}, respectively; Fig. 2). This contrasts with the biomass dominance of tubular *Ulva* observed in the field. In this sense, higher transportation rates of biomass (removal from the bay to the open sea) expected for the free-living laminar morphologies of *Ulva* (Schories and Reise 1993, Salomonsen et al. 1997, Bermejo et al. 2019) and the more frequent generalized sporulation or bleaching events observed for laminar morphologies (e.g., Hiraoka 2021) may account for this.

Comparing the results observed with similar studies assessing the growth of *Ulva compressa* under similar experimental conditions, this study yielded much lower values for the RGR than those observed by Wang et al. (2018; between 0.25 and 0.20 · d^{-1}) or Løvlie (1969; 0.3–0.5 · d^{-1}), but similar to results obtained by Taylor et al. (2001; 0.05–0.08 · d^{-1}) and Lotze and Schramm (2000; 0.09–0.11 · d^{-1}). Regarding *U. lacinulata*, the growth rates were similar to the ones obtained by Gao et al. (2016a; 0.10–0.15 · d^{-1}) and Rautenberger et al. (2015; 0.08–0.22 · d^{-1}) for specimens of this species incubated under similar conditions. These differences in growth observed between experiments in the case of *U. compressa* could be a result of differences in culture methodologies (water motion, culture media, or light quality and quantity), thallus age (e.g., Gao et al. 2016a), or in the biological performances of strains of *U. compressa* (e.g., Løvlie 1969, Fort et al. 2020). Further experiments considering standardized methodologies would be necessary in

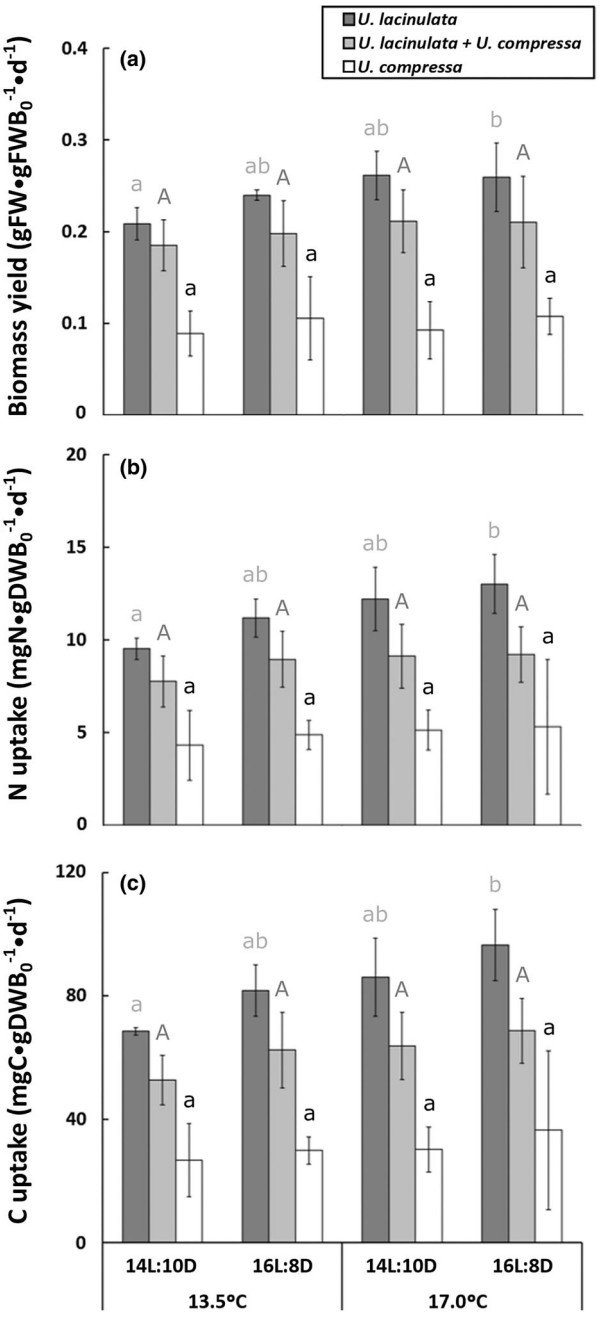

FIG. 4. Biomass yield, N and C uptake of *Ulva compressa*, *U. lacinulata*, and co-cultures of both species under four different combinations of temperature (13.5°C and 17°C) and photoperiod (14:10 h light:dark and 16:8 h light:dark) conditions. Data represent mean ± standard deviation ($n = 4$). Letters over the bars represent significant differences between treatments according to the Tukey test. The different colors of the letters over the bars indicate that post hoc comparisons between treatments were performed for each type of culture (*U. lacinulata* monoculture—light gray lowercase letter; *U. compressa* monoculture—black lowercase letter; co-culture of *U. lacinulata* and *U. compressa*—black capital letter).

order to unravel the key factor explaining these differences, which seems to be more important in the case of *U. compressa* than for *U. lacinulata*.

Assuming the scenario of global warming proposed by the IPCC for early summer (i.e., June) in the year 2070 and the expected increase in nutrients loadings in Irish estuaries (O'Boyle et al. 2017), the results obtained support the idea of a change in the structure and seasonality of green tides. This agrees with the results of Gao et al. (2016a), who predicted an increase in green tides dominated by *Ulva lacinulata* in the context of global warming and eutrophication based on laboratory studies. In this case, it is expected that an earlier development in the summer of *U. lacinulata* blooms might increase the total biomass of *Ulva* per square meter at this time of the year due to the simultaneous occurrence of the peak bloom of tubular and laminar morphologies. Moreover, if the duration of the *U. lacinulata* blooming season is also extended, this could enhance the exportation of *Ulva* biomass, as laminar morphologies are more prone to exportation out of the estuary (Schories and Reise 1993, Bermejo et al. 2019). Increased biomass exportation of *Ulva* could have a positive local impact in estuaries, having a similar effect to the removal of seaweed biomass.

The biotic interactions between these two species in the context of no-nutrient limitation were neutral (i.e., *Ulva compressa*) or positive (i.e., *U. lacinulata*). Regarding the growth of *U. lacinulata*, it seems to be enhanced by the presence of *U. compressa* (Fig. 3). Fong et al. (1996), in a scenario of nutrient deprivation, found that *U. expansa* facilitated the growth of *U. intestinalis*, which was attributed to the release of dissolved organic nitrogen (DON) when *U. expansa* was limited by nitrogen. Although the release of DON cannot be ruled out as the mechanism explaining this facilitation, no N limitation was observed during the experiment since the media were replaced every 2 d and the tissue N in both species was higher than 4%, which is almost the double of the critical quota estimated for similar *Ulva* species (>2.45%; Pedersen and Borum 1996, Villares and Carballeira 2004). Thus, since other variables (e.g., the presence of allelopathic compounds, DON, DOP and DOC) were not measured during the development of the experiment, the mechanisms regulating this interaction remain unexplained. On this matter, further studies should assess the interactions between these species in the context of nutrient limitation, since non-linear responses could occur. All these possibilities are of high relevance for the development of successful management strategies.

Finally, the results indicated that the coculture of *Ulva compressa* and *U. lacinulata* under eutrophic conditions showed averaging values of biomass yield, N and C uptake when compared with monospecific cultures of both species (Fig. 4). Considering the weak biotic interaction observed between these species (neutral or slightly synergistic effect; Fig. 3), their different response to environmental fluctuations (Tables 1 and 2), and its similar function in the community, these results suggest that the

persistence and stability of green tides could be enhanced by an increase in the number of opportunistic species able to produce macroalgal blooms, as explained by the diversity-stability hypothesis (McCann 2000). The increasing number of studies reporting the coexistence of several species in green tides (Guidone et al. 2013, Bermejo et al. 2019, Kang et al. 2019), the occurrence of temporal and spatial successions between bloom-forming species as a result of environmental gradients or disturbances (Lavery et al. 1991, Nelson et al. 2008), or the increased extension of macroalgal blooms due to the arrival of alien species (Yabe et al. 2009, Bermejo et al. 2020) also support this hypothesis. The understanding of the biotic interaction, positive and negative, between these species, and the density dependent mechanisms regulating their interactions (e.g., competition for resources, allelopathic compounds, and mutual protection) will be useful for the implementation of effective suitable environmental management strategies or for *Ulva* aquaculture, as this species is cultivated for commercial or bioremediation purposes (e.g., IMTA). In the case of seaweed aquaculture, the co-culture of different *Ulva* species showing weak species interactions and different performances under specific disturbances might enhance yield stability (e.g., Haughey et al. 2018), especially when culture conditions cannot be controlled.

This work has been co-financed under the 2014-2020 EPA Research Strategy (Environmental Protection Agency, Ireland), project no: 2015-W-MS-20 (the Sea-MAT Project) and project no: 2018-W-MS-32 (the MACRO-MAN Project), the 2014-2020 ERDF Operational Programme and by the Department of Economy, Knowledge, Business and University of the Regional Government of Andalusia (Project reference: FEDER-UCA18-106875), the INNOVALGA Project of the Spanish Ministry of Agriculture, Fisheries and Food, and the University of Cadiz throughout the mobility program "Atracción talento: Jóvenes Investigadores" (Ref: UCA/R22REC/2017). Funding for open access provided by University of Malaga / CBUA. The authors are thankful to Moya O'Donnell and Claudia L. Cara for laboratory assistance.

Airoldi, L. & Beck, M. W. 2007. Loss, status and trends for coastal marine habitats of Europe. *Oceanogr. Mar. Biol. An Annu. Rev.* 45:345–405.

Allanson, B. R., Human, L. R. D. & Claassens, L. 2016. Observations on the distribution and abundance of a green tide along an intertidal shore, Knysna Estuary. *South African J. Bot.* 107:49–54.

Bartsch, I., Wiencke, C. & Laepple, T. 2012. Global Seaweed Biogeography Under a Changing Climate: The Prospected Effects of Temperature. *In* Wiencke, C. & Bischof, K. [Eds.] *Seaweed Biology*. Springer-Verlag, Berlin Heidelberg, pp. 471–93.

Bermejo, R., Golden, N., Schrofner, E., Knöller, K., Fenton, O., Serrão, E. & Morrison, L. 2022. Biomass and nutrient dynamics of major green tides in Ireland: Implications for biomonitoring. *Mar. Pollut. Bull.* 175:113318.

Bermejo, R., Heesch, S., Mac Monagail, M., O'Donnell, M., Daly, E., Wilkes, R. J. & Morrison, L. 2019. Spatial and temporal variability of biomass and composition of green tides in Ireland. *Harmful Algae* 81:94–105.

Bermejo, R., MacMonagail, M., Heesch, S., Mendes, A., Edwards, M., Fenton, O., Knöller, K., Daly, E. & Morrison, L. 2020. The arrival of a red invasive seaweed to a nutrient over-enriched estuary increases the spatial extent of macroalgal blooms. *Mar. Environ. Res.* 158:104944.

Bi, H. & Turvey, N. D. 1994. Inter-specific competition between seedlings of *Pinus radiata*, *Eucalyptus regnans* and *Acacia melanoxylon*. *Aust. J. Bot.* 42:61–70.

Brodie, J. A., Maggs, C. A. & John, D. M. 2007. *Green seaweeds of Britain and Ireland*. British Phycological Society, London, 520 pp.

Camill, P. 2010. Global change. *Nat. Educ. Knowl.* 3:49.

Casado-Amezúa, P., Araújo, R., Bárbara, I., Bermejo, R., Borja, Á., Díez, I., Fernández, C. et al. 2019. Distributional shifts of canopy-forming seaweeds from the Atlantic coast of Southern Europe. *Biodivers. Conserv.* 28:1151–72.

Coffaro, G. & Bocci, M. 1997. Resources competition between *Ulva rigida* and *Zostera marina*: a quantitative approach applied to the Lagoon of Venice. *Ecol. Model.* 102:81–95.

Coll, M., Piroddi, C., Steenbeek, J., Kaschner, K., Ben Rais Lasram, F., Aguzzi, J., Ballesteros, E. et al. 2010. The biodiversity of the Mediterranean Sea: estimates, patterns, and threats. *PLoS ONE* 5:e11842.

Costanza, R., d'Arge, R., de Groot, R., Farber, S., Grasso, M., Hannon, B., Limburg, K. et al. 1997. The value of the world's ecosystem services and natural capital. *Nature* 387:253–60.

Darriba, D., Posada, D., Kozlov, A. M., Stamatakis, A., Morel, B. & Flouri, T. 2020. ModelTest-NG: A New and Scalable Tool for the Selection of DNA and Protein Evolutionary Models. *Mol. Biol. Evol.* 37:291–4.

Edler, D., Klein, J., Antonelli, A. & Silvestro, D. 2021. raxmlGUI 2.0: A graphical interface and toolkit for phylogenetic analyses using RAxML. *Methods Ecol Evol.* 12:373–7.

Fletcher, R. L. 1996. The occurrence of "green tides" - a review. *In* Schramm, W. & Nienhuis, P. H. [Eds.] *Marine Benthic Vegetation: Recent Changes and the Effects of Eutrophication*. Springer, Berlin, Germany, pp. 7–43.

Fong, P., Boyer, K. E., Desmond, J. S. & Zelder, J. B. 1996. Salinity stress, nitrogen competition and facilitation: what controls seasonal succession of 2 opportunistic green macroalgae? *J. Exp. Mar. Bio. Ecol.* 206:203–21.

Fort, A., Linderhof, C., Coca-Tagarro, I., Inaba, M., McHale, M., Cascella, K., Potin, P., Guiry, M. D. & Sulpice, R. 2021. A sequencing-free assay for foliose *Ulva* species identification, hybrid detection and bulk biomass characterisation. *Algal Res.* 55:102280.

Fort, A., Mannion, C., Fariñas-Franco, J. M. & Sulpice, R. 2020. Green tides select for fast expanding *Ulva* strains. *Sci. Total Environ.* 698:134337.

Gao, G., Clare, A. S., Rose, C. & Caldwell, G. S. 2016a. Eutrophication and warming-driven green tides (*Ulva rigida*) are predicted to increase under future climate change scenarios. *Mar. Pollut. Bull.* 114:439–47.

Gao, G., Zhong, Z., Zhou, X. & Xu, J. 2016b. Changes in morphological plasticity of *Ulva prolifera* under different environmental conditions: A laboratory experiment. *Harmful Algae* 59:51–8.

Gattuso, J. P., Magnan, A., Billé, R., Cheung, W. W. L., Howes, E. L., Joos, F., Allemand, D. et al. 2015. Contrasting futures for ocean and society from different anthropogenic CO_2 emissions scenarios. *Science* 349:aac4722.

Glez-Peña, D., Gómez-Blanco, D., Reboiro-Jato, M., Fdez-Riverola, F. & Posada, D. 2010. ALTER: program-oriented format conversion of DNA and protein alignments. *Nucleic Acids Res.* 38: W14–8.

Glibert, P. M. 2017. Eutrophication, harmful algae and biodiversity — Challenging paradigms in a world of complex nutrient changes. *Mar. Pollut. Bull.* 124:591–606.

Griekspoor A. & Groothuis T. 2015. 4Peaks. https://www.nucleobytes.com/

Guidone, M., Thornber, C., Wysor, B. & O'Kelly, C. J. 2013. Molecular and morphological diversity of Narragansett Bay (RI, USA) *Ulva* (Ulvales, Chlorophyta) populations. *J. Phycol.* 49:979–95.

Guidone, M. & Thornber, C. S. 2013. Examination of *Ulva* bloom species richness and relative abundance reveals two cryptically co-occurring bloom species in Narragansett Bay, Rhode Island. *Harmful Algae* 24:1–9.

Guillard, R. 1975. Culture of phytoplankton for feeding marine invertebrates. *In* Smith, W. L. & Chanley, M. H. [Eds.] *Culture of Marine Invertebrate Animals*. Plenum Press, New York, USA, pp. 26–60.

Haughey, E., Suter, M., Hofer, D., Hoekstra, N. J., McElwain, J. C., Lüscher, A. & Finn, J. A. 2018. Higher species richness enhances yield stability in intensively managed grasslands with experimental disturbance. *Sci. Rep.* 8:1–10.

Hayden, H. S., Blomster, J., Maggs, C. A., Silva, P. C., Stanhope, M. J. & Waaland, J. R. 2003. Linnaeus was right all along: *Ulva* and *Enteromorpha* are not distinct genera. *Eur. J. Phycol.* 38:277–94.

Heesch, S., Broom, J. E. S., Neill, K. F., Farr, T. J., Dalen, J. L. & Nelson, W. A. 2009. *Ulva, Umbraulva* and *Gemina*: Genetic survey of New Zealand taxa reveals diversity and introduced species. *Eur. J. Phycol.* 44:143–54.

Heesch, S., Pažoutová, M., Moniz, M. B. J. & Rindi, F. 2016. Prasiolales (Trebouxiophyceae, Chlorophyta) of the Svalbard Archipelago: diversity, biogeography and description of the new genera *Prasionella* and *Prasionema*. *Eur. J. Phycol.* 51:171–87.

Hernandez, I., Peralta, G., Perez-Llorens, J. L., Vergara, J. J. & Niell, F. X. 1997. Biomass and growth dynamics of *Ulva* species in Palmones River estuary. *J. Phycol.* 33:764–72.

Hiraoka, M. 2021. Massive *Ulva* green tides caused by inhibition of biomass allocation to sporulation. *Plan. Theory* 10:2482.

Hughey, J. R., Gabrielson, P. W., Maggs, C. A. & Mineur, F. 2022. Genomic analysis of the lectotype specimens of European *Ulva rigida* and *Ulva lacinulata* (Ulvaceae, Chlorophyta) reveals the ongoing misapplication of names. *Eur. J. Phycol.* 57:143–53.

Hughey, J. R., Maggs, C. A., Mineur, F. & Gabrielson, P. W. 2019. Genetic analysis of the Linnaean *Ulva lactuca* (Ulvales, Chlorophyta) holotype and related type specimens reveals name missapplications, unexpected origins, and new synonomies. *J. Phycol.* 55:503–8.

IPCC 2021. Climate Change 2021: The Physical Science Basis, the Working Group I contribution to the Sixth Assessment Report on 6 August 2021 during the 14th Session of Working Group I and 54th Session of the IPCC.

Jeffrey, D. W., Brennan, M. T., Jennings, E., Madden, B. & Wilson, J. G. 1995. Nutrient sources for in-shore nuisance macroalgae: The dublin bay case. *Ophelia* 42:147–61.

Kang, J. H., Jang, J. E., Kim, J. H., Byeon, S. Y., Kim, S., Choi, S. K., Kang, Y. H., Park, S. R. & Lee, H. J. 2019. Species composition, diversity, and distribution of the genus *Ulva* along the coast of Jeju Island, Korea based on molecular phylogenetic analysis. *PLoS ONE* 14:e0219958.

Kozlov, A. M., Darriba, D., Flouri, T., Morel, B. & Stamatakis, A. 2019. RAxML-NG: a fast, scalable and user-friendly tool for maximum likelihood phylogenetic inference. *Bioinformatics* 35:4453–5.

Krause-Jensen, D., Sagert, S., Schubert, H. & Boström, C. 2008. Empirical relationships linking distribution and abundance of marine vegetation to eutrophication. *Ecol. Indic.* 8:515–29.

Lakens, D. 2013. Calculating and reporting effect sizes to facilitate cumulative science: A practical primer for t-tests and ANOVAs. *Front. Psychol.* 4:1–12.

Lavery, P. S., Lukatelich, R. J. & McComb, A. J. 1991. Changes in the biomass and species composition of macroalgae in a eutrophic estuary. *Estuar. Coast. Shelf Sci.* 33:1–22.

Le Moal, M., Gascuel-Odoux, C., Ménesguen, A., Souchon, Y., Étrillard, C., Levain, A., Moatar, F., Pannard, A., Souchu, P., Lefebvre, A. & Pinay, G. 2019. Eutrophication: A new wine in an old bottle? *Sci. Total Environ.* 651:1–11.

Leal, P. P., Ojeda, J., Sotomayor, C. & Buschmann, A. H. 2020. Physiological stress modulates epiphyte (*Rhizoclonium* sp.)-basiphyte (*Agarophyton chilense*) interaction in co-culture under different light regimes. *J. Appl. Phycol.* 32:3219–32.

Lenzi, M., Gennaro, P., Renzi, M., Persia, E. & Porrello, S. 2012. Spread of *Alsidium corallinum* C. Ag. in a Tyrrhenian eutrophic lagoon dominated by opportunistic macroalgae. *Mar. Pollut. Bull.* 64:2699–707.

Lotze, H. K., Lenihan, H. S., Bourque, B. J., Bradbury, R. H., Cooke, R. G., Kay, M. C., Kidwell, S. M., Kirby, M. X., Peterson, C. H. & Jackson, J. B. C. 2006. Depletion, degradation, and recovery potential of estuaries and coastal seas. *Science* 312:1806–9.

Lotze, H. K. & Schramm, W. 2000. Ecophysiological traits explain species dominance patterns in macroalgal blooms. *J. Phycol.* 295:287–95.

Løvlie, A. 1969. Cell size, nucleic acids, and synthetic efficiency in the wild type and a growth mutant of the multicellular alga *Ulva mutabilis* Fyøn. *Dev. Biol.* 20:349–67.

Lüning, K. 1990. *Seaweeds: their environment, biogeography, and ecophysiology*. John Wiley & Sons, Inc, Hoboken, New Jersey, 527 pp.

Malta, E. J., Draisma, S. G. A. & Kamermans, P. 1999. Free-floating *Ulva* in the southwest Netherlands: species or morphotypes? A morphological, molecular and ecological comparison. *Eur. J. Phycol.* 34:443–54.

McCann, K. S. 2000. The diversity–stability debate. *Nature* 405:228–33.

Müller K., Müller J., Neinhuis C. & Quandt D. 2010. PhyDE: Phylogenetic data editor, version 0.9971. http://www.phyde.de.

Nelson, T. A., Haberlin, K., Nelson, A. V., Ribarich, H., Hotchkiss, R., Van Alstyne, K. L., Buckingham, L., Simunds, D. J. & Fredrickson, K. 2008. Ecological and physiological controls of species composition in green macroalgal blooms. *Ecology* 89:1287–98.

Nelson, T. A., Nelson, A. V. & Tjoelker, M. 2003. Seasonal and spatial patterns of "green tides" (Ulvoid algal blooms) and related water quality parameters in the coastal waters of Washington state, USA. *Bot. Mar.* 46:263–75.

O'Boyle, S., Wilkes, R., Mcdermott, G. & Ní Longphuirt, S. 2017. Will recent improvements in estuarine water quality in Ireland be compromised by plans for increased agricultural production? A case study of the Blackwater estuary in southern Ireland. *Ocean Coast. Manag.* 143:87–95.

Pedersen, M. F. & Borum, J. 1996. Nutrient control of algal growth in estuarine waters. Nutrient limitation and the importance of nitrogen requirements and nitrogen storage among phytoplankton and species of macroalgae. *Mar. Ecol. Prog. Ser.* 142:261–72.

Poloczanska, E. S., Smith, S., Fauconnet, L., Healy, J., Tibbetts, I. R., Burrows, M. T. & Richardson, A. J. 2011. Little change in the distribution of rocky shore faunal communities on the Australian east coast after 50 years of rapid warming. *J. Exp. Mar. Bio. Ecol.* 400:145–54.

R Core Team 2017. *R: A language and environment for statistical computing*. R Foundation for Statistical Computing, Vienna, Austria URL https://www.R-project.org/.

Rambaut, A. 2016. *FigTree v.* Institute fo Evolutionary Biology, University of Edinburgh, Edinburgh, UK http://www.tree.bio.ed.ac.uk/software/figtree/.

Rautenberger, R., Fernández, P., Strittmatter, M., Heesch, S., Cornwall, C. E., Hurd, C. L. & Roleda, M. Y. 2015. Saturating light and not increased carbon dioxide under ocean acidification drives photosynthesis and growth in *Ulva rigida* (Chlorophyta). *Ecol. Evol.* 5:874–88.

Salomonsen, J., Flindt, M. R. & Geertz-Hansen, O. 1997. Significance of advective transport of *Ulva lactuca* for a biomass budget on a shallow water location. *Ecol. Model.* 102:129–32.

Schories, D. & Reise, K. 1993. Germination and anchorage of *Enteromorpha* spp. in sediments of the Wadden Sea. *Helgoländer Meeresuntersuchungen*. 47:275–85.

Smetacek, V. & Zingone, A. 2013. Green and golden seaweed tides on the rise. *Nature* 504:84–8.

Stamatakis, A. 2014. RAxML version 8: a tool for phylogenetic analysis and post-analysis of large phylogenies. *Bioinformatics* 30:1312–3.

Steinhagen, S., Karez, R. & Weinberger, F. 2019. Cryptic, alien and lost species: molecular diversity of *Ulva* sensu lato along

the German coasts of the North and Baltic Seas. *Eur. J. Phycol.* 54:466–83.
Taylor, R., Fletcher, R. & Raven, J. 2001. Preliminary studies on the growth of selected "green tide" algae in laboratory culture: effects of irradiance, temperature, salinity and nutrients on growth rate. *Bot. Mar.* 44:327–36.
Teichberg, M., Fox, S. E., Olsen, Y. S., Valiela, I., Martinetto, P., Iribarne, O., Muto, E. Y. et al. 2010. Eutrophication and macroalgal blooms in temperate and tropical coastal waters: Nutrient enrichment experiments with *Ulva* spp. *Glob. Chang. Biol.* 16:2624–37.
UN 2021. Global Population Growth and Sustainable Development. UN DESA/POP/2021/TR/NO. 2.
Valiela, I., Mcclelland, J., Hauxwell, J., Behr, P. J., Hersh, D. & Foreman, K. 1997. Macroalgal blooms in shallow estuaries: Controls and ecophysiological and ecosystem consequences. *Limnol. Oceanogr.* 42:1105–18.
Vergara, J. J., Lucas, J. P., Peralta, G., Hernandez, I. & Niell, F. X. 1997. Seasonal variation of photosynthetic performance and light attenuation in *Ulva* canopies from Palmones river estuary. *J. Phycol.* 779:773–9.
Villares, R. & Carballeira, A. 2004. Nutrient limitation in macroalgae (*Ulva* and *Enteromorpha*) from the Rías Baixas (NW Spain). *Mar. Ecol.* 25:225–43.
Wan, A. H. L., Wilkes, R. J., Heesch, S., Bermejo, R., Johnson, M. P. & Morrison, L. 2017. Assessment and characterisation of Ireland's green tides (*Ulva* species). *PLoS ONE* 12:e0169049.
Wang, S., Huo, Y., Zhang, J., Cui, J., Wang, Y., Yang, L., Zhou, Q., Lu, Y., Yu, K. & He, P. 2018. Variations of dominant free-floating *Ulva* species in the source area for the world's largest macroalgal blooms, China: Differences of ecological tolerance. *Harmful Algae* 74:58–66.
Wang, Y., Wang, Y., Zhu, L., Zhou, B. & Tang, X. 2012. Comparative studies on the ecophysiological differences of two green tide macroalgae under controlled laboratory conditions. *PLoS ONE* 7:e38245.
Wang, Z., Xiao, J., Fan, S., Li, Y., Liu, X. & Liu, D. 2015. Who made the world's largest green tide in China?—an integrated study on the initiation and early development of the green tide in yellow sea. *Limnol. Oceanogr.* 60:1105–17.
Wernberg, T., Russell, B. D., Thomsen, M. S., Gurgel, C. F. D., Bradshaw, C. J. A., Poloczanska, E. S. & Connell, S. D. 2011. Seaweed communities in retreat from ocean warming. *Curr. Biol.* 21:1828–32.
Worm, B., Lotze, H. K., Boström, C., Engkvist, R., Labanauskas, V. & Sommer, U. 1999. Marine diversity shift linked to interactions among grazers, nutrients and propagule banks. *Mar. Ecol. Prog. Ser.* 185:309–14.
Yabe, T., Ishii, Y., Amano, Y., Koga, T., Hayashi, S. & Nohara, S. 2009. Green tide formed by free-floating *Ulva* spp. at Yatsu tidal flat, Japan. *Limnology* 10:239–45.

Supporting Information

Additional Supporting Information may be found in the online version of this article at the publisher's web site:

Figure S1. Phylogenetic tree inferred by maximum-likelihood analysis from partial *rbc*L sequences of Ulvacean species. The numbers above branches indicate ML bootstrap support values, with values below 60% not shown. Species names (reflecting current nomenclature; Guiry and Guiry 2022) are followed by GenBank accession numbers, the origin of the sample, and a number indicating the reference: 1- Fort et al. (2022); 2- Hayden and Waaland (2004); 3- Hayden et al. (2003); 4- Heesch et al. (2009); 5- Heesch et al. (2021); 6- Hiraoka et al. (2003); 7- Ichihara et al. (2013); 8- Ichihara et al. (2015); 9- Kawai et al. (2021); 10- Kirkendale et al. (2013); 11- Kraft et al. (2010); 12- Krupnik et al. (2018); 13- Loughnane et al. (2008); 14- Mares et al. (2011); 15- Massocato et al. (2022); 16- Ogawa et al. (2013); 17- Saunders and Kucera (2010); 18- Shimada et al. (2003); 19- Spalding et al. (2016); and 20- this study (new sequences set in bold).

Table S1. Mean ± standard deviation values of relative growth rate (RGR; d^{-1}), tissue N (%), tissue C (%), and water content (WC; %) for *Ulva compressa* and *U. lacinulata* cultivated under different conditions of temperature (Temp; °C), photoperiod (L:D; h), and biotic interaction (BI; monoculture -Mono- or co-culture -Co-cult-).